STRUCTURAL BEHAVIOR OF REINFORCED CONCRETE CONTINUOUS DEEP BEAMS WITH WEB OPENINGS

By

: Keun-Hyeok Yang[*,**], BSc, MSc, PhD, Archi. Engng

and Ashraf F. Ashour, BSc, MSc, PhD, CEng, MIStructE

K. H. Yang is currently a visiting research fellow at the University of Bradford, UK and an assistant professor at Mokpo National University, Korea. He received his MSc and PhD degrees from Chungang University, Korea. His research interests include ductility, strengthening and shear of reinforced high-strength concrete structures.

A.F.Ashour is a senior lecturer at the University of Bradford, UK. He obtained his BSc and MSc degrees from Mansoura University, Egypt and his PhD from Cambridge University, UK. His research interests include shear, plasticity, repair and strengthening and optimisation of reinforced concrete and masonry structures.

Keywords : Beams & girders, Buildings, structures & design, Concrete structures.

Total number of words : 4900

Total number of figures :10

Total number of tables : 3

ABSTRACT

[*] Corresponding author, Department of Architectural Engineering, Mokpo National University, Mokpo, Jeonnam, South Korea, Tel: +82 (0)61 450 2456, Fax: +82 (0)61 450 6454, E-mail: *yangkh@mokpo.ac.kr* (current Tel : +44 (0) 1274 23 4163)

Ten reinforced concrete continuous deep beams with openings were tested to failure. The main variables investigated were the shear span-to-overall depth ratio, and the size and location of openings. Two failure modes influenced by the size and location of web openings regardless of the shear span-to-overall depth ratio were observed. The normalized load capacity of beams having a web opening area ratio of 0.025 within exterior shear spans were approximately similar to that of their companion solid beams. Continuous deep beams having web openings within interior shear spans exhibited a higher load capacity reduction with the increase of the opening size, similar to simply supported deep beams with web openings. Formulas based on the upper bound analysis of the plasticity theory were proposed to predict the load capacity of continuous deep beams with web openings. Comparisons between the measured and predicted load capacities showed a good agreement.

Keywords: continuous deep beams, openings, failure mode, load capacity, upper-bound analysis.

INTRODUCTION

Openings are frequently placed in the web area of reinforced concrete deep beams to facilitate essential services, such as ventilating ducts, water supply and drainage pipes, network access or even movement from one room to another. Most of the existing investigations[1-5] on deep beams with web openings focused on simply supported deep beams. However, reinforced concrete deep beams are commonly supported on several supports and, consequently, high shear and high moment coincide within interior shear spans where failure usually occurs. Ashour and Rishi[6] reported test results of 16 reinforced concrete deep beams with web openings, having a shear span-to-overall depth ratio of 1.08. They concluded that web openings within interior shear spans caused more reduction to the beam capacity than those within exterior shear spans and vertical web reinforcement was more effective than horizontal web reinforcement. However, very few, if any,

tests of continuous deep beams with web openings having a shear span-to-overall depth ratio less than 1.0 were published. Furthermore, their design guidelines have not been provided yet by most code provisions[7-11].

This paper presents test results of eight two-span reinforced concrete deep beams with web openings and two companion solid deep beams. The main variables considered were the shear span-to-overall depth ratio, and the size and location of openings. Formulas based on the upper-bound plasticity theory, considering different failure modes observed in accordance with the size and location of openings are proposed.

RESEARCH SIGNIFICANCE

There is very few, if any, published data available on the influence of web openings on the structural behaviour of continuous deep beams having shear span-to-overall depth ratio less than 1.0. Test results reported in the present study clearly show that the failure mode and load capacity of continuous deep beams with web openings, which are significantly dependent on the size and location of openings, are completely different from those in simple deep beams with openings. In addition, the normalized shear capacity of continuous deep beams with web openings was higher than that of simple deep beams with web openings. The difference was more prominent when the shear span-to-overall depth ratio was 0.6 rather than 1.0

EXPERIMENTAL INVESTIGATION

The details of geometrical dimensions and longitudinal reinforcement of test specimens are shown in Table 1 and Fig. 1. Two sizes of web openings, $0.25a \times 0.1h$ and $0.5a \times 0.2h$, where a and h are the shear span and overall section depth, respectively, were investigated according to the variation of the opening location and shear span-to-overall depth ratio. For web opening sizes of

$0.25a \times 0.1h$ and $0.5a \times 0.2h$, the ratios, ρ_{OA}, of opening area to the shear span area are 0.025 and 0.1, respectively. The shear span-to-overall depth ratios, a/h, were selected as 0.6 and 1.0. The web openings were located either in exterior shear spans or in interior shear spans as shown in Fig. 2. In each beam tested, the opening center was positioned in accordance with that of the shear span area to completely interrupt the natural load path joining the load and support as shown in Fig. 2. The beam notation given in Table 1 includes four parts except the two companion solid deep beams, 6N and 10N. The first part is used to identify the shear span-to-overall depth ratio: '6' for a/h=0.6 and '10' for a/h=1.0. The second part refers to the opening location: 'E' for web openings within exterior shear spans and 'I' for web openings within interior shear spans. The third part gives the width of web openings: 'T' for $0.25a$ and 'F' for $0.5a$. The last part explains the depth of web openings: '1' for $0.1h$ and '2' for $0.2h$. For example, the notation 6ET1 means a continuous deep beam having shear span-to-overall depth ratio of 0.6 and web opening size of $0.25a \times 0.1h$ within exterior shear spans.

All tested beams had the same section width, b_w, of 160 mm, and overall depth, h, of 600 mm. Three steel bars of 19 mm diameter, and 560 MPa yield strength were used for either longitudinal top or bottom reinforcement. As a result, the longitudinal top, $\rho_s^{'}\left(=\frac{A_s^{'}}{b_w d}\right)$, and bottom, $\rho_s\left(=\frac{A_s}{b_w d}\right)$, reinforcement ratios were 1% in all beams tested. The clear cover to longitudinal top and bottom reinforcement was 35 mm. The longitudinal bottom reinforcement was continuous over the full length of the beam and welded to 160×100×10 mm end plates. The longitudinal top reinforcement was anchored in the outside of the exterior support by 90° hook according to ACI 318-05 as shown in Fig. 1. To examine the influence of openings on continuous deep beams, no shear reinforcement was provided. Design concrete strength was 60 MPa. Cylinders of 100 mm

diameter × 200 mm high were cast and cured simultaneously with beams to determine the compressive strength of concrete.

Test set-up

Loading and instrumentation arrangements are shown in Fig. 2. All beams having two spans were tested to failure under a symmetrical two-point top loading system with a loading rate of 30 kN/min using a 3000 kN capacity universal testing machine (UTM). Each span was identified as E-Span or W-span as shown in Fig. 2. The two exterior end supports are designed to allow horizontal and rotational movements, whereas the intermediate support prevents horizontal movement but allows rotation. In order to evaluate the shear force and loading distribution, 1000 kN capacity load cells were installed in both exterior end supports. At the location of loading or support point, a steel plate of 100 mm, 150 mm or 200 mm wide was provided to prevent premature crushing or bearing failure as shown in Fig. 2. All beams were preloaded up to a total load of 150 kN before testing, which wouldn't produce any cracks, in order to assure a similar loading distribution to supports according to the result of a linear two-dimensional finite element (2-D FE) analysis.

Vertical deflections at mid-span of each span and settlements at both intermediate and end supports were measured using linear variable differential transformers (LVDTs). The PI type gages were used for measuring diagonal crack width at concrete struts as shown in Fig. 2. The test data were captured by a data logger and automatically stored.

EXPERIMENTAL RESULTS AND DISCUSSION

Support settlements

Continuous deep beams are sensitive to differential support settlements causing additional moment and shear. The measured support settlements of test specimens having a/h=0.6 and opening size of

$0.5a \times 0.2h$ against the total applied load are given in Fig. 3: Fig. 3 (a) for beam 6EF2 having openings within exterior shear spans, and Fig. 3 (b) for beam 6IF2 having openings within interior shear spans. Until the occurrence of the first diagonal crack, the measured end support settlement was similar to that at the intermediate support. However, after the first diagonal crack, for beam 6EF2 having web openings within exterior shear spans, the settlement at the intermediate support was increased compared with that at the end support and the differential support settlement reached about $L/17000$ at failure load. Whereas the measured intermediate support settlement was less than that at the end support for beam 6IF2 having web openings within interior shear spans; the maximum differential support settlement was $L/21000$. A linear 2-D FE analysis was conducted to assess the effect of differential support settlement recorded on the reaction distribution of the above two beams. It shows that the additional end and intermediate support reactions are 17.5 kN (4.1% of that at failure) and 35.5 kN (2.1% of that at failure), respectively, due to $L/17000$ differential support settlement of beam 6EF2, and 6.5 kN (1.4% of that at failure) and 15.4 kN (1.9% of that at failure), respectively, due to $L/21000$ differential support settlement of beam 6IF2. This indicates that the differential support settlement due to the current test set-up has a very little effect on the redistribution of internal stresses and development of additional moment and shear.

Crack propagation and failure modes

The first cracking load and crack propagation of continuous deep beams with web openings were influenced by the shear span-to-overall depth ratio, and size and location of openings as shown in Table 2 and Fig. 4. Just before failure, crack patterns above and below openings were nearly similar. A symmetrical crack pattern was also observed for both E and W spans of the deep beams tested before failure. The first crack in all beams tested except solid beams occurred at opening corners near load points (at B and D in Fig. 2) and propagated toward load points with the load increase. The crack propagation around openings in continuous deep beams was very similar to that in simple

deep beams with web openings tested by Kong and Sharp[1] and Yang et al.[5] For beams having web openings within exterior shear spans, flexural cracks in hogging and sagging zones occurred almost simultaneously with a diagonal crack within the interior shear span after the occurrence of diagonal cracks around exterior openings. For beams having web openings within interior shear spans, most cracks concentrated at corners of openings and diagonal cracks at exterior shear spans didn't appear in case of beams having a/h=1.0.

The failure mode of beams having openings within exterior shear spans was strongly dependent on the opening size regardless of the shear span-to-overall depth ratio. For beams having small openings (ρ_{OA}=0.025) within exterior shear spans, failure planes formed along the main interior diagonal strut joining the edges of load and intermediate support plates similar to the companion solid deep beams. Whereas, the failure of beams having large openings (ρ_{OA}=0.1) within exterior shear spans occurred at both interior and exterior shear spans as shown in Fig. 4. On the other hand, the failure plane of beams having web openings within interior shear spans formed along diagonal concrete struts joining the edges of the load plates and opening corners opposite to the load points, AE and CF in Fig. 2. (b), regardless of the opening size and shear span-to-overall depth ratio.

Load versus mid-span deflection

The mid-span deflections at the failed span for different beams tested against the total applied load are shown in Fig. 5: Fig. 5 (a) for beams having a/h=0.6 and Fig. 5 (b) for beams having a/h=1.0. The initial stiffness of beams with openings was similar to that of the companion solid deep beams, regardless of location and size of openings. After the first diagonal crack appeared at web opening corners, the deflection of beams sharply increased. This increase rate of deflection was more prominent with the increase of the opening size and the shear span-to-depth ratio. Openings within interior shear spans caused a higher stiffness reduction than those within exterior shear spans.

Support reaction

Fig. 6 shows the amount of the load transferred to the intermediate and end supports against the total applied load: Fig. 6 (a) for beams having a/h=0.6 and Fig. 6 (b) for beams having a/h=1.0. On the same figure, the support reactions in companion solid deep beams obtained from a linear 2-D FE analysis are also presented. For continuous solid deep beams, test specimens 6N and 10 N, the measured support reactions showed good agreement with those predicted by the linear 2-D FE analysis. Whereas, the occurrence of the first diagonal crack caused large discrepancy in support reactions of continuous deep beams with web openings and their companion solid deep beams. For beams having web openings within interior shear spans, the amount of load transferred to end supports increased and the intermediate support reaction decreased relative to those of the companion solid deep beams or predictions obtained from the linear 2-D FE analysis. On the other hand, end support reactions reduced for beams having web openings within exterior shear spans. These differences between continuous deep beams with web openings and their companion solid deep beams in support reactions increased with the increase of web opening size, but seemed to be independent on the shear span-to-overall depth ratio.

Diagonal crack width

Fig. 7 shows the development of maximum diagonal crack width for all beams tested against the total applied load. In each beam tested except the companion solid deep beams and beams 6ET1 and 10ET1 having small openings (ρ_{OA} = 0.025) within exterior shear spans, the maximum diagonal crack width was in the lower load path CF (openings within interior shear spans) or CG (openings within exterior shear spans) connecting the edge of the support plate and the opening corner opposite to the support as shown in Fig. 2 similar to the case of simple deep beams[5]. On the other hand, the maximum crack width of companion solid deep beams and beams 6ET1 and 10ET1 was measured in the natural load path EF joining the edges of load and intermediate support plates as

shown in Fig. 2 (a). The relation between the diagonal crack width and applied load in beams having small openings (ρ_{OA} = 0.025) within exterior shear spans was quite similar to that in companion solid deep beams until just before failure. Whereas, for beams having web openings within interior shear spans or large openings (ρ_{OA} = 0.1) within exterior shear spans, the diagonal crack width reached the limit crack width of 0.4mm specified for serviceability of concrete members in ACI 318-02[7] as soon as the diagonal crack occurred. In addition, the increasing rate of diagonal crack width against the applied load was more notable with the increase of the shear span-to-overall depth ratio and the opening size.

Load and shear capacities

The influence of the opening area ratio, ρ_{OA}, on the normalized load capacity, $\lambda_n = \frac{P_n}{2b_w h\sqrt{f_c'}}$, of test specimens is plotted in Fig. 8 and given in Table 2, where P_n is the total applied load. Fig. 9 also shows the effect of the opening area ratio, ρ_{OA}, on the normalized shear capacity, $\eta_n = \frac{V_n}{b_w h\sqrt{f_c'}}$, at the failed shear span of test specimens, where V_n is the shear force at failure. Experimental results of continuous deep beams with web openings tested by Ashour and Rishi[6] and simple deep beams with web openings similar to those in the present study in the material and geometrical properties tested by Yang et al.[5] are also given in Fig. 8 and Fig. 9. In case of simple deep beams, the normalized load capacity is estimated from $\frac{P_n}{b_w h\sqrt{f_c'}}$. The normalized load and shear capacities were greatly influenced by the size and location of openings and failure mechanism. For beams having an opening area ratio of 0.025 within exterior shear spans, the normalized load and shear capacities were approximately similar to those of the companion solid continuous deep beams, as their failure planes were formed along the major diagonal concrete struts joining the

edges of load and intermediate support plates as shown in Fig. 4. Even beam 10ET1 failed at a normalized load capacity slightly higher than that of the companion solid beam 10N. The load capacity of the beams tested by Ashour and Rishi was slightly higher than that of the solid beam, 10N, as shown in Fig. 8(b). This may be attributed to the web reinforcement used in the beams tested by Ashour and Rishi. The normalized load capacity of beams having openings within exterior shear spans was higher than that of both beams having openings within interior shear spans and simple deep beams with openings. However, the normalized shear capacity at the failed shear span of beams 6EF2 and 10EF2 having large openings within exterior shear spans was similar to that of beams having openings within interior shear spans as shown in Fig. 9 and Table 2. In Fig. 9, as the failure in the two beams 6ET1 and 10ET1 occurred within the interior shear spans, therefore, the exterior openings had no effect on the shear capacity which was almost similar to that of the companion solid beams. For beams having openings within interior shear spans, the normalized load and shear capacities decreased with the increase of the opening area ratio, as expected. The decreasing rate was nearly similar to that in simple deep beams with openings regardless of the shear span-to-overall depth ratio. On the other hand, the normalized shear capacity of continuous deep beams with web openings was higher than that of simple deep beams with web openings.

Upper-bound analysis for load capacity

Mechanisms of failure

The two failure mechanisms ascertained in the present study and also observed in Ashour and Rishi's work are analyzed using the upper-bound analysis of the plasticity theory. Each failure mechanism is idealized as an assemblage of rigid blocks separated by yield lines as proposed by Ashour and Rishi[6], and Ashour and Morley[12]. Failure mechanisms with a failure plane formed at the interior shear span only and at both interior and exterior shear spans are identified as failure modes

A and B, respectively, as given in Table 2 and shown in Fig. 10. For beams having web openings within exterior shear spans, the failure mode seems to be dependent on the opening area ratio. In tests carried out by Ashour and Rishi[6], beams having an opening area ratio more than 0.037 within exterior shear spans failed in failure mode B as observed in the current tests for beams 6EF2 and 10EF2 (ρ_{OA} = 0.1). However, beams tested in the current investigation having an opening area ratio of 0.025 within exterior shear spans exhibited failure mode A as shown in Fig. 10 (b). Therefore, it may be suggested that there is a web opening area ratio between 0.025 and 0.037 at which the failure mechanism would be changed from mode A to mode B for continuous deep beams with openings within exterior shear spans.

Material Modelling

Concrete is assumed to be a rigid perfectly plastic material with the modified Coulomb failure criteria[13] as yield condition. The tensile strength is ignored and the effective compressive strength, f_c^*, is

$$f_c^* = \nu_e f_c' \tag{1}$$

where ν_e = effectiveness factor and f_c' = cylinder compressive strength of concrete. Both top and bottom chords above and below openings in deep beams are considered to be in a state of biaxial tension-compression. In the present study, Vecchio and Collins's[14] model for the effectiveness factor is adopted to consider the discrepancy of transverse tensile strains between upper and lower yield lines as follows:

$$\nu_e = \frac{1}{1.0 + K_c K_f}$$

$$K_c = 0.35\left(-\frac{\varepsilon_1}{\varepsilon_3} - 0.28\right)^{0.8} \geq 1.0 \tag{2}$$

$$K_f = 0.1825\sqrt{f_c'} \geq 1.0$$

where ε_1 and ε_3 = the principal tensile and compressive strains in the yield line, respectively. As the principal strains $\varepsilon_{1,3}$ is $\frac{1}{2}\frac{\delta}{\Delta}(\sin\alpha \pm 1)$ in the yield line having discontinuous width of Δ from the plasticity theory, $-\frac{\varepsilon_1}{\varepsilon_3}$ in the factor K_c can be written as $\frac{1+\sin\alpha}{1-\sin\alpha}$, where α = angle between the relative displacement δ at the midpoint of the chord and yield line as shown in Fig. 10.

Tensile and compressive reinforcing steel bars are assumed to be a rigid perfectly plastic material with yield strength, f_y.

Load capacity equation for beams failed in mode A

Fig. 10 (a) for beams having web openings within interior shear spans and Fig. 10 (b) for beams with openings of area ratio less than 0.025~0.037 within exterior shear spans show the idealized failure mechanisms based on test results. Continuous deep beams with openings collapsed in mode A can be usually idealized as an assemblage of two rigid blocks separated by a yield line. Rigid block *I* undergoes a relative rotation around an instantaneous center (I.C.), which is similar to that observed for continuous deep beams without openings as proposed by Ashour and Morley[15]. On the other hand, rigid block *II* is fixed over the intermediate and other end supports. Jensen[16] proved that the optimal shape of the yield line is a hyperbola with orthogonal asymptotes through I.C. to achieve a stationery value of the total energy dissipation as shown in Fig. 10 (a) and (b). The yield line turns into a straight line when the I.C. approaches infinity.

The upper-bound theorem of the plasticity theory is based on the energy principle of equating the total internal energy, W_I, to the external work, W_E. The total internal energy commonly depends on the position of the I.C. and the amount of internal stress in both concrete along the yield line and reinforcing bars crossing the yield line. Since the relative displacement rate, δ_i, equals $\omega \cdot r_i$, where subscript i identifies the number of yield lines, ω and r_i indicate relative rotational displacement

of rigid block *II* about the I.C. and distance between the midpoint of the chord of the yield line i and I.C., respectively, as shown in Fig. 10 (a).

For continuous deep beams having web openings within interior shear spans, at failure, both of the upper and lower yield lines seldom have the same displacement rate and angle about I.C. It was shown by Nielsen[13] and Marti[17] that the energy dissipated by concrete along the hyperbolic yield line could be calculated using details of the straight line between the ends of the hyperbolic yield line as shown in Fig. 10 (a) and Fig. 10 (b). Therefore, the energy W_c dissipated in concrete is[6, 13]

$$W_c = \frac{1}{2} b_w f_c^{'} \omega \sum_{i=1}^{2} \left[(v_e)_i r_i (1 - \sin \alpha_i) L_i \right] \tag{3}$$

where α_i = angle between the relative displacement δ_i at the midpoint of the chord and yield line i, and L_i = the length of the yield line i.

For continuous deep beams having an opening area ratio less than 0.025~0.037 within exterior shear spans, the concrete energy dissipated in yield line 3 shown in Fig. 10 (b) is

$$W_c = \frac{1}{2} b_w f_c^{'} \omega \left[(v_e)_3 r_3 (1 - \sin \alpha_3) L_3 \right] \tag{4}$$

Because the relative displacement of each reinforcing bar, $(\delta_s)_j$, can be written as $\omega \cdot (r_s)_j$, where $(r_s)_j$ = distance between the intersection point of reinforcing bar j with yield line and the I.C., the energy, W_s, dissipated in all reinforcement crossing the yield line is calculated from[6, 12]

$$W_s = \omega \sum_{j=1}^{n} (A_s)_j (f_y)_j (r_s)_j \cos(\alpha_s)_j \tag{5}$$

where n = number of reinforcing bars crossing the yield line, $(A_s)_j$, and $(f_y)_j$ = area and yield strength of the reinforcing bar j crossing the yield line, respectively, and $(\alpha_s)_j$ = angle between the relative displacement δ_s about the I.C. and the reinforcing bar j crossing the yield line.

The external work, W_E, done by the vertical load $P_n / 2$ on rigid block *I* in Fig. 10. (a) and (b) is

$$W_E = \frac{P_n}{2}\omega|a - X_{ic}| \tag{6}$$

where a = shear span which is the distance between the load point and exterior support, and X_{ic} = the horizontal coordinate of the I.C. Equating the total internal energy dissipated in concrete and reinforcement to the external work done, the load capacity, P_n, can be written in the following form:

For beams having web openings within interior shear spans:

$$P_n = \frac{f_c' b_w h}{|a - X_{ic}|}\left[\sum_{i=1}^{2}[(v_e)_i r_i(1-\sin\alpha_i)L_i] + 2\sum_{j=1}^{n}(\phi_s)_j (r_s)_j \cos(\alpha_s)_j\right] \tag{7. a}$$

For beams having openings of area ratio less than 0.025~0.037 within exterior shear spans:

$$P_n = \frac{f_c' b_w h}{|a - X_{ic}|}\left[(v_e)_3 r_3(1-\sin\alpha_3)L_3 + 2\sum_{j=1}^{n}(\phi_s)_j (r_s)_j \cos(\alpha_s)_j\right] \tag{7.b}$$

where $(\phi_s)_j = \frac{(A_s)_j (f_y)_j}{b_w h f_c'}$ = reinforcement index for each individual reinforcing bar j crossing the yield line. The load capacity is implicitly expressed as a function of the position of the instantaneous center (X_{ic}, Y_{ic}) as given in Eq. (7). The horizontal coordinate, X_{ic}, of the instantaneous center coincide with that of the global coordinates since the vertical displacement of rigid block I is prevented at the exterior support as shown in Fig. 10 (a) and Fig. 10 (b). According to the upper-bound theorem, collapse occurs at the least strength. The minimum value of strength is obtained by varying the vertical coordinate, Y_{ic}, of the instantaneous center along the vertical axis of the global coordinate.

Load capacity equation for beams failed in mode B

The idealized failure mechanism for continuous deep beams having openings of area ratio exceeding 0.037 within exterior shear spans is given in Fig. 10 (c). As proposed by Ashour and Rishi[6], at failure, it consists of three rigid blocks separated by three yield lines. It can be generally assumed that the central block, rigid block *II*, vertically moves by an amount δ, and the other two blocks, rigid block *I* and rigid block *III*, are fixed over supports as observed in the beam testing. Therefore, the energy dissipated in concrete is

$$W_c = \frac{1}{2} b_w f_c' \delta \sum_{i=1}^{3} \left[(v_e)_i (1 - \cos \beta_i) L_i \right] \tag{8}$$

where β_i = angle between the yield line i and longitudinal axis of beam. There is no energy dissipated in horizontal reinforcement, as only vertical movement exists in the yield line. The energy, W_s, dissipated in vertical reinforcing bars crossing the yield line is calculated from:

$$W_s = \delta \sum_{j=1}^{n} (A_v)_j (f_{yv})_j \tag{9}$$

where $(A_v)_j$, and $(f_{yv})_j$ = area and yield strength of the vertical reinforcing bar j crossing the yield line, respectively, and n = number of reinforcing bars crossing the two yield lines.

The external work done by the vertical load on the moving block *II* is

$$W_E = \frac{P_n}{2} \delta \tag{10}$$

Equating the internal energy dissipation to the external work done, the load capacity predicted by failure mechanism B is

$$P_n = b_w h f_c' \left[\sum_{i=1}^{3} \left\{ (v_e)_i (1 - \cos \beta_i) \frac{L_i}{h} \right\} + 2 \sum_{j=1}^{n} (\phi_{sv})_j \right] \tag{11}$$

where $(\phi_{sv})_j = \dfrac{(A_v)_j (f_{yv})_j}{b_w h f_c'}$ = vertical reinforcement index for the individual bar j crossing the yield line.

Comparison of predicted and experimental failure loads

To examine the validity of the proposed model, comparisons between the predictions and experimental results of the load capacity, P_n, are given in Table 3: Table 3 (a) for beams collapsed in mode A shown in Fig. 10 (a) or Fig. 10 (b) and Table 3 (b) for beams failed in mode B shown in Fig. 10 (c). The details and results of continuous deep beams with web openings tested by Ashour and Rishi[6] are also presented in Table 3. For beams having failure mode A, the mean and standard deviation of the ratio between the predicted and experimental load capacities $(P_n)_{Pro.}/(P_n)_{Exp.}$ are 1.08 and 0.21, respectively. For beams A-I-S and A-I-L tested by Ashour and Rishi, which have a large amount of vertical and horizontal shear reinforcing bars, the predictions obtained from Eq. (7.a) highly overestimate the test results as all shear reinforcement crossing yield lines would not be yielded at failure as assumed in Eq. (7). Excluding these two specimens, A-I-S and A-I-L, the mean and standard deviation are 1.02 and 0.12, respectively. For beams having openings of area ratio greater than 0.037 within exterior shear spans, the mean and standard deviation are 1.01 and 0.12, respectively. Equations (7) and (11) would overestimate the collapse load of beams tested as they are based on the upper bound analysis of the plasticity theory. However, the load capacity of several beams was underestimated, which implies that more internal energy is being dissipated. This is mainly attributed to the fact that the internal energy dissipated in concrete is dependent on the effectiveness factor v_e. This indicates that a slightly higher effectiveness factor would be used. The predictions obtained from Eq. (7) and Eq. (11) presented by mechanism analysis show good agreement with experimental results.

CONCLUSIONS

To study the influence of the size and location of web openings on the behaviour of reinforced concrete continuous deep beams, ten beams were tested. The following conclusions may be drawn:

1. Two failure modes influenced by the size and location of web openings were observed, regardless of the shear span-to-overall depth ratio. The transition of the failure mode for beams having web openings within exterior shear spans was strongly dependent on the ratio of opening area to shear span area.
2. Lager diagonal crack width appeared in beams having web openings within interior shear spans than in beams having web openings within exterior shear spans which showed the closest diagonal crack width to that of their companion solid beams.
3. The normalized load and shear capacities for beams having openings of area ratio of 0.025 within exterior shear spans were approximately similar to those of their companion solid beams.
4. Both continuous deep beams having web openings within interior shear spans and simple deep beams with web openings are practically similar in the decreasing rate of the normalized load capacity against the increase of the opening area ratio.
5. The normalized load capacity of beams having openings within exterior shear spans was higher than that of both continuous beams having openings within interior shear spans and simple deep beams with openings.
6. The normalized shear capacity of continuous deep beams with web openings was slightly higher than that of simple deep beams with the same web opening size. The difference was more prominent when the shear span-to-overall depth ratio was 0.6 rather than 1.0.
7. The formulas proposed to predict the load capacity of continuous deep beams with web openings showed a good agreement with test results.

ACKNOWLEDGMENTS

This work was supported by the Korea Research Foundation Grant (KRF-2003-041-D00586) and the Regional Research Centers Program (Bio-housing Research Institute), granted by the Korean Ministry of Education & Human Resources Development. The authors wish to express their gratitude for financial support.

NOTATION

A_{st} area of longitudinal bottom reinforcement

$A_{st}^{'}$ area of longitudinal top reinforcement

a shear span distance measured from center of support to center of loading point

b_w width of beam

d effective depth of beam

$f_c^{'}$ cylinder compressive strength of concrete

f_c^{*} effective strength of concrete

f_y yield strength of reinforcement

h overall depth of beam

m_1, m_2 coefficient of opening size

P_{cr} the first diagonal crack load

P_{fl} initial flexural crack load

P_n load capacity

r distance between the midpoint of the chord of the yield line and the instantaneous center

V_{cr} the first diagonal crack shear force

V_n shear force

v_e effective strength factor

W_c internal energy dissipated in concrete

W_E external work done by applied load

W_I total internal energy dissipated in yield line

W_s internal energy dissipated in reinforcement

α angle between the relative displacement at the midpoints of the chord and yield line

β angle between yield line and longitudinal axis.

δ relative displacement vector across a yield line

η_n normalized shear capacity at failed shear span $\left(= V_n / b_w h\sqrt{f_c^{'}}\right)$

λ_n normalized load capacity $\left(= P_n / 2b_w h\sqrt{f_c^{'}}\right)$

ρ_{OA} the ratio of opening area to the shear span area

ρ_s longitudinal bottom reinforcement ratio ($= A_{st} / b_w d$)

$\rho_s^{'}$ longitudinal top reinforcement ratio ($= A_{st}^{'} / b_w d$)

ω relative rotational displacement of rigid block I

REFERENCES

1. Kong, F. K., and Sharp, G. R., “Shear Strength of Light Weight Reinforced Concrete Deep Beams with Web Openings,” The Structural Engineer, V. 51, No. 8, Aug. 1973, pp. 267-275.

2. Kong, F. K., Sharp, G. R., Appleton, S. C., Beaumont C. J., and Kubik, L. A., “Structural Idealization for Deep Beams with Web Openings; Further Evidence,” Magazine of Concrete Research, V. 30, No. 103, June 1978, pp. 89-95.

3. Tan, K. H., Tong, K., and Tang, C. Y., “Consistent Strut-and-Tie modelling of Deep Beams with Web Openings,” Magazine of Concrete Research, V. 55, No. 1, Feb. 2003, pp. 65-75.

4. 3. Tan, K. H., Tang, C. Y., and Tong, K., “Shear Strength Predictions of Pierced Deep Beams with Inclined Web Reinforcement,” Magazine of Concrete Research, V. 56, No. 8, Aug. 2004, pp. 443-352.

5. Yang, K. H., Eun, H, C, and Chung, H. S., "The Influence of Web Openings on the Structural Behavior of Reinforced High-Strength Concrete Deep Beams,” Engineering Structures, Accepted, 2006.

6. Ashour, A. F., and Rishi, G., “Tests of Reinforced Concrete Continuous Deep Beams with Web Openings,” ACI Structural Journal, V. 97, No. 3, May-June 2000, pp. 418-426.

7. ACI Committee 318: Building Code Requirements for Structural Concrete (ACI 318-02) and Commentary (ACI 318R-02). American Concrete Institute, 2002.

8. ACI Committee 318: Building Code Requirements for Structural Concrete (ACI 318-05) and Commentary (ACI 318R-05). American Concrete Institute, 2005.

9. Canadian CSA Building Code, Design of Concrete Structures: Structures (Design)-A National Standard of Canada (CAN-A23.3-94), Clause 11.1.2, Canadian Standards Association. Toronto, 1994.

10. CEB-FIP MC 90, Design of Concrete Structures. CEB-FIP Model Code 1990, Thomas Telfore, London, 1993.

11. CIRIA, The Design of Deep Beams in Reinforced Concrete (CIRIA 2). Ove Arup & Partners and CIRIA, London, 1997.

12. Ashour, A. F., and Morley, C. T., "The Numerical Determination of Shear Failure Mechanisms in Reinforced Concrete Beams", The Structural Engineer, V. 72, No. 23 & 24, Dec. 1994, pp. 395-400.

13. Nielsen, M. P., Limit Analysis and Concrete Plasticity, Prentice-Hall, Englewood Cliffs, 1984.

14. Vecchio, F. J., and Collins, M. P., "Compression Response of Cracked Reinforced Concrete", Journal of Structural Engineering ASCE, V. 119, No. 12, Dec. 1993, pp. 3590-3610.

15. Ashour, A. F., and Morley, C. T., "Effectiveness Factor of Concrete in Continuous Deep Beams," Journal of Structural Engineering, ASCE, V. 122, No. 2, Feb. 1996, pp. 169-178.

16. Jensen, J. F., "Discussion of 'An Upper-Bound Rigid-Plastic Solution for the Shear Failure of Concrete Beams without Shear Reinforcement,' by K. O. Kemp, and M. T. Al-Safi." Magazine of Concrete Research, V. 34, No. 119, 1982, pp. 100-103.

17. Marti, P., "Basic Tools of Reinforced Concrete Beam Design," ACI Structural Journal, V. 82, No. 1, 1985, pp. 46-56.

TABLES AND FIGURES

List of Tables:

Table 1 – Details of test specimens

Table 2 – Details of test results

Table 3 – Basic data and comparison between experimental and theoretical load capacity

List of Figures:

Fig. 1 – Specimen details and arrangement of longitudinal reinforcement.

Fig. 2 – Test setup.

Fig. 3 – Support deflection against total applied load.

Fig. 4 – Crack patterns and failure of beams tested.

Fig. 5 – Mid-span deflection against total applied load.

Fig. 6 – Support reaction against total applied load.

Fig. 7 – Maximum diagonal crack width against total applied load.

Fig. 8 – Relationship between ρ_{OA} and λ_n.

Fig. 9 – Relationship between ρ_{OA} and η_n.

Fig. 10 – Idealization of failure mechanism for continuous deep beams with web openings.

Table 1–Details of test specimens

Speci-men	f_c' (MPa)	a/h	a (mm)	L (mm)	Opening details					
					Location	Width		Depth		ρ_{OA}
						m_1	$m_1 a$ (mm)	m_2	$m_2 h$ (mm)	
6N	60.7	0.6	360	720	Solid	-	-	-	-	-
6ET1	68.2				Exterior shear spans	0.25	90	0.1	60	0.025
6EF2						0.5	180	0.2	120	0.1
6IT1					Interior shear spans	0.25	90	0.1	60	0.025
6IF2						0.5	180	0.2	120	0.1
10N	48.1	1.0	600	1200	Solid	-	-	-	-	-
10ET1	60.7				Exterior shear spans	0.25	150	0.1	60	0.025
10EF2	68.2					0.5	300	0.2	120	0.1
10IT1					Interior shear spans	0.25	150	0.1	60	0.025
10IF2						0.5	300	0.2	120	0.1

Note : f_c' = cylinder compressive strength, a/h = shear span-to-overall depth ratio, a = shear span, L = one span length, m_1 = ratio of opening width to shear span, m_2 = ratio of opening depth to overall section depth, h = overall section depth, and ρ_{OA} = ratio of opening area to shear span area.

Table 2-Details of test results

Speci-men	Initial flexural cracking load P_{fl} (kN)			Load (P_{cr}) and shear force (V_{cr}) at the first diagonal crack, (kN)								Failure load (P_n) and shear force (V_n) at failed interior shear span, (kN)				Failure mode
	Hogging zone.	Sagging zone		W-span				E-span				P_n	$\lambda_n = \frac{P_n/2}{b_w h\sqrt{f_c'}}$	V_n	$\eta_n = \frac{V_n}{b_w h\sqrt{f_c'}}$	
		W-span	E-span	Interior		Exterior		Interior		Exterior						
				P_{cr}	V_{cr}	P_{cr}	V_{cr}	P_{cr}	V_{cr}	P_{cr}	V_{cr}					
6N	1405	990	918	1250	369	2260	574	1090	328	2260	566	2860	1.91	828	1.11	A
6ET1	1190	1150	1160	1093	351	794	163	1170	394	1117	183	2649	1.67	860	1.08	A
6EF2	1140	1030	1046	1090	385	759	122	1490	523	806	127	2499	1.58	857(443*)	1.08(0.56)	B
6IT1	1040	990	867	674	195	2130	615	760	218	2130	615	2199	1.39	615	0.77	A
6IF2	907	769	860	530	140	1710	404	417	118	-	-	1716	1.08	406	0.51	A
10N	459	793	791	600	207	-	-	600	203	-	-	1208	0.91	388	0.58	A
10ET1	460	550	520	640	210	480	75	770	266	620	108	1402	0.94	485	0.65	A
10EF2	496	520	500	626	258	410	149	967	366	410	145	1207	0.76	444(159*)	0.56(0.20)	B
10IT1	479	551	616	325	103	-	-	412	123	-	-	1325	0.84	393	0.50	A
10IF2	312	269	264	175	55	-	-	214	64	-	-	874	0.55	194	0.24	A

* shear force at failed exterior shear span

Table 3- Basic data and comparison between experimental and theoretical load capacity

(a) For beams collapsed in failure mode A

Researchers	Specimen	b_w, mm	h, mm	f_c', MPa	a/h	Details of openings				Longitudinal reinforcement		Shear reinforcement		P_n		$\frac{(P_n)_{Pro.}}{(P_n)_{Exp.}}$
						m_1	m_2	ρ_{OA}	Position	Top	Bottom	Horizontal	Vertical	Exp.	Pro.	
Present study	6N	160	600	60.7	0.6	-	-	-	Solid	3ϕ19	3ϕ19	-	-	2860	2408	0.84
	6ET1			68.2		0.25	0.1	0.025	Ext.					2649	2491	0.94
	6IT1			68.2		0.25	0.2	0.025	Int.					2199	2172	0.99
	6IF2			68.2		0.5	0.2	0.1	Int.					2145	1799	1.05
	10N			48.1	1.0	-	-	-	Solid					1208	1356	1.12
	10ET1			60.7		0.25	0.1	0.025	Ext.					1402	1452	1.04
	10IT1			68.2		0.25	0.2	0.025	Int.					1325	1200	0.91
	10IF2			68.2		0.5	0.2	0.1	Int.					874	952	1.09
Ashour and Rishi	A-I-S	120	625	20.8	1.08	0.18	0.2	0.037	Int.	4ϕ12+ 2ϕ10	4ϕ12	8ϕ8	29ϕ8	588	800	1.36
	A-I-L			26.1		0.37	0.4	0.147						418	706	1.69
	B-I-S			26.1		0.18	0.2	0.037				4ϕ8	15ϕ8	684	634	0.93
	B-I-L			25.3		0.37	0.4	0.147						374	480	1.28
	C-I-S			22.9		0.18	0.2	0.037				4ϕ8	-	516	520	1.01
	C-I-L			23.9		0.37	0.4	0.147						329	368	1.12
	D-I-S			25.5		0.18	0.2	0.037				-	15ϕ8	659	592	0.90
	D-I-L			26.2		0.37	0.4	0.147						383	422	1.10
Mean																1.08
Std.																0.21

(b) For beams collapsed in failure mode B

Researchers	Specimen	b_w, mm	h, mm	f_c', MPa	a/h	Details of openings				Longitudinal reinforcement		Shear reinforcement		P_n		$\frac{(P_n)_{Pro.}}{(P_n)_{Exp.}}$
						m_1	m_2	ρ_{OA}	Position	Top	Bottom	Horizontal	Vertical	Exp.	Pro.	
Present study	6EF2	160	600	68.2	0.6	0.5	0.2	0.1	Ext.	3ϕ19	3ϕ19	-	-	2499	2514	1.01
	10EF2				1.0									1207	1428	1.18
Ashour and Rishi	A-E-S	120	625	26.5	1.08	0.18	0.2	0.037	Ext.	4ϕ12+ 2ϕ10	4ϕ12	8-ϕ8	29ϕ8	902	1050	1.16
	A-E-L			29.8		0.37	0.4	0.147						863	982	1.14
	B-E-S			26.4		0.18	0.2	0.037				4-ϕ8	15ϕ8	865	840	0.97
	B-E-L			26.9		0.37	0.4	0.147						739	710	0.96
	C-E-S			24.7		0.18	0.2	0.037				4-ϕ8	-	648	592	0.91
	C-E-L			25.0		0.37	0.4	0.147						598	476	0.79
	D-E-S			24.7		0.18	0.2	0.037				-	15ϕ8	797	800	1.00
	D-E-L			28.1		0.37	0.4	0.147						753	742	0.98
Mean																1.01
Std.																0.12

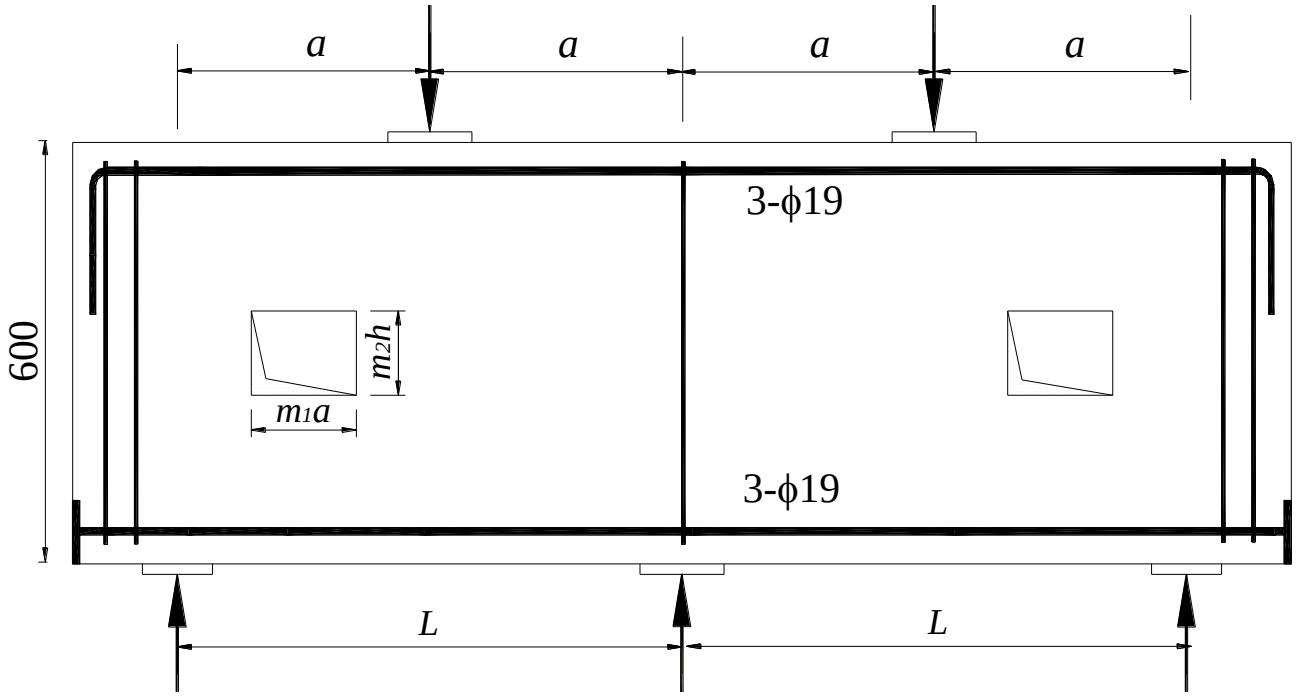

Fig. 1-Specimen details and arrangement of longitudinal reinforcement.

(all dimensions are in mm)

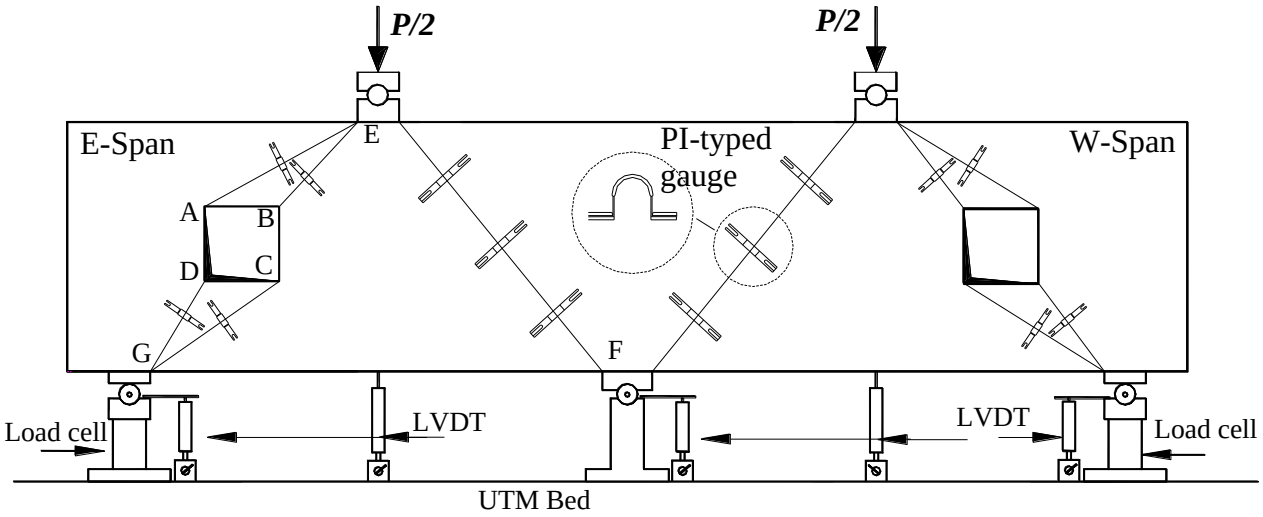

(a) Beams having web openings within exterior shear spans

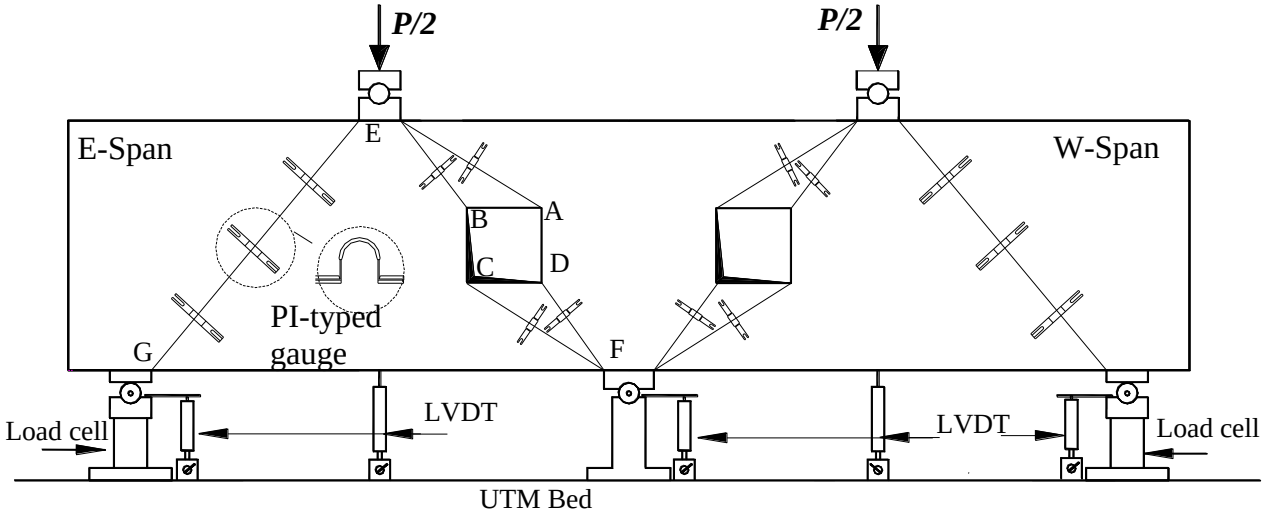

(b) Beams having web openings within interior shear spans

Fig. 2-Test setup (all dimensions are in mm).

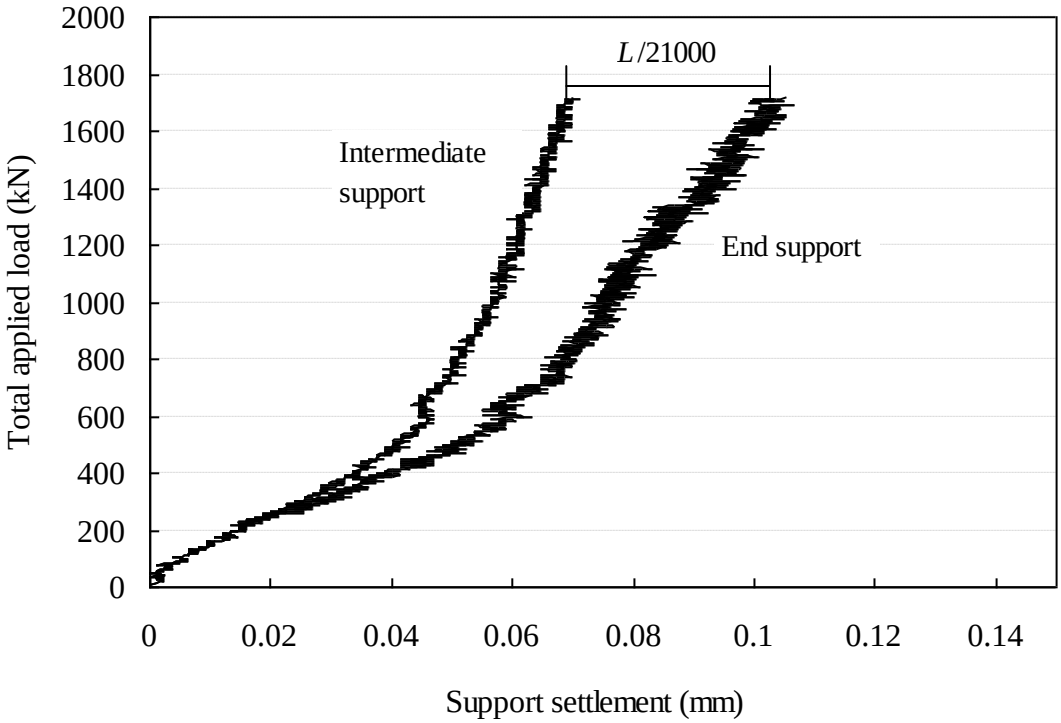

(a) 6EF2 (Beam having web openings within exterior shear spans)

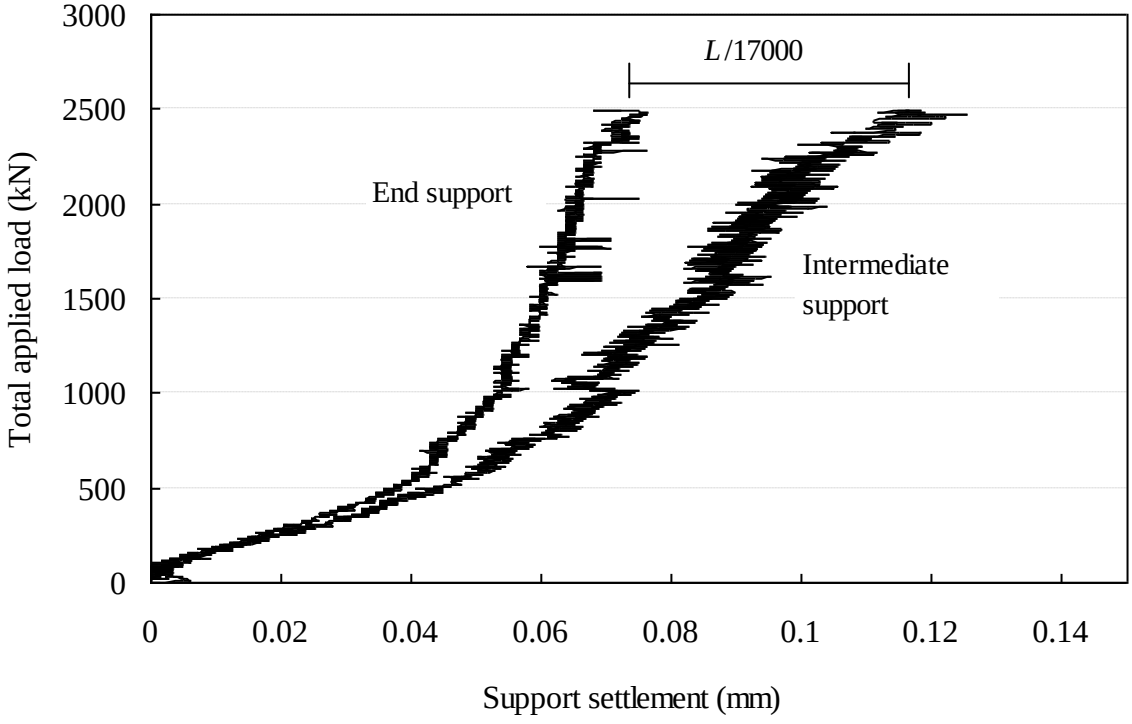

(b) 6IF2 (Beam having web openings within interior shear spans)

Fig. 3-Support deflection against total applied load.

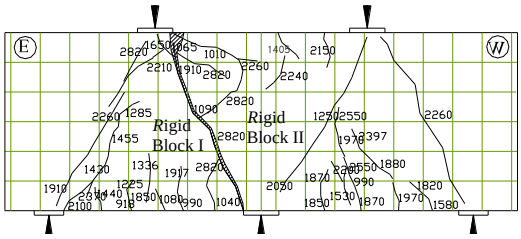

(a) 6N

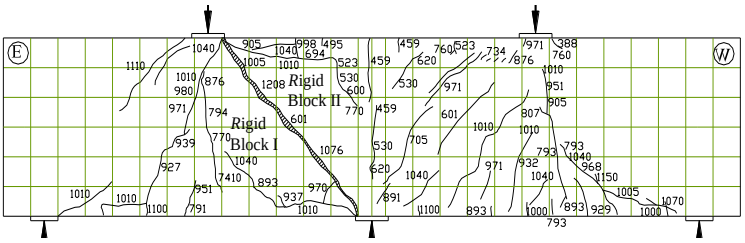

(f) 10N

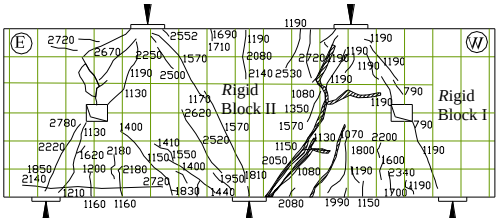

(b) 6ET1

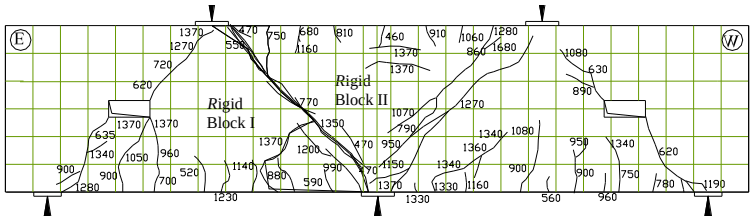

(g) 10ET1

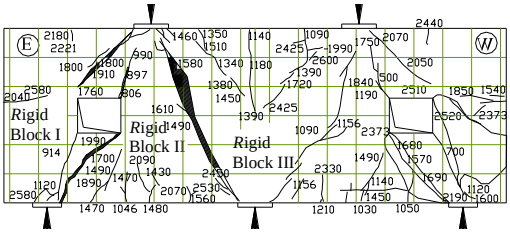

(c) 6EF2

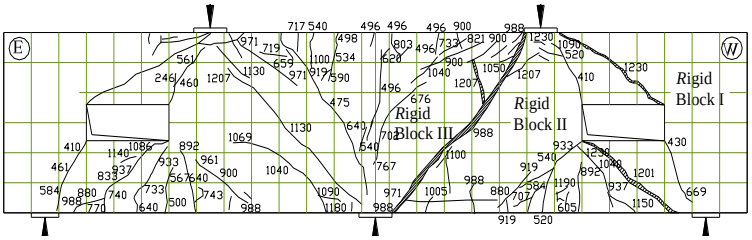

(h) 10EF2

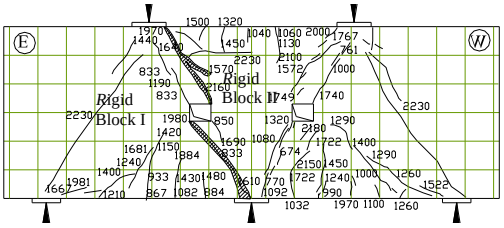

(d) 6IT1

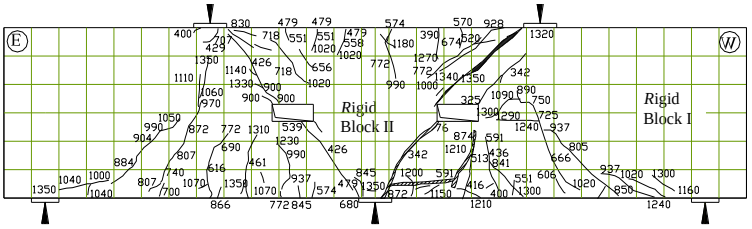

(i) 10IT1

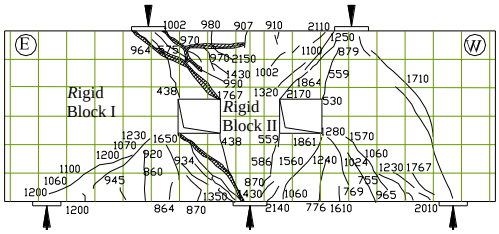

(e) 6IF2

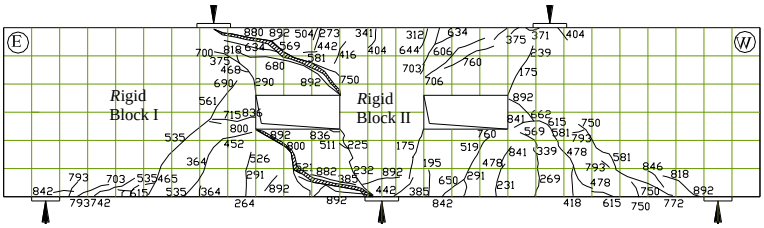

(j) 10IF2

Fig. 4–Crack patterns and failure of beams tested

(Numbers indicate the total load in kN at which crack occurred.)

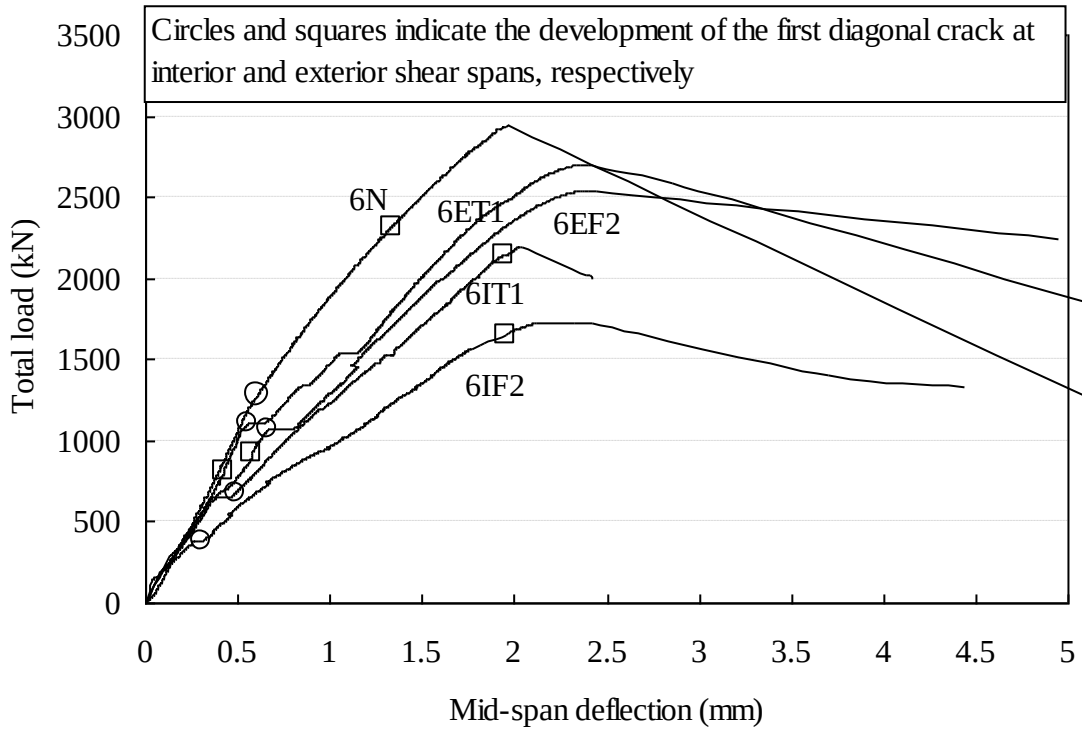

(a) a/h = 0.6

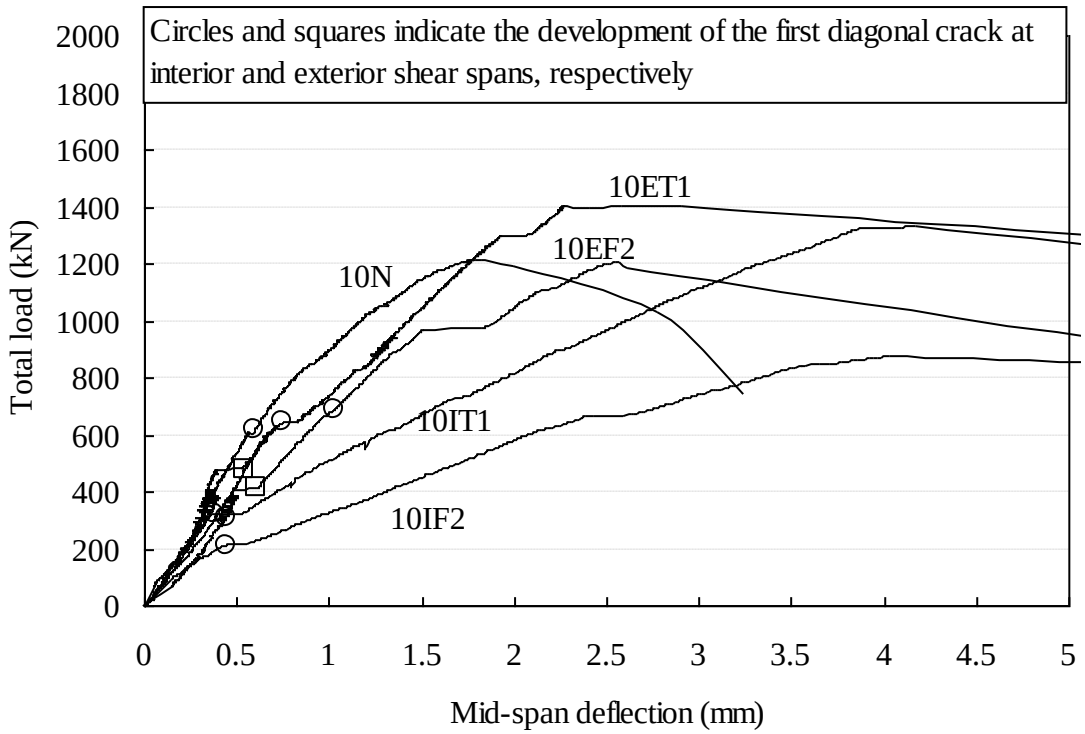

(b) a/h = 1.0

Fig. 5–Mid-span deflection against total applied load.

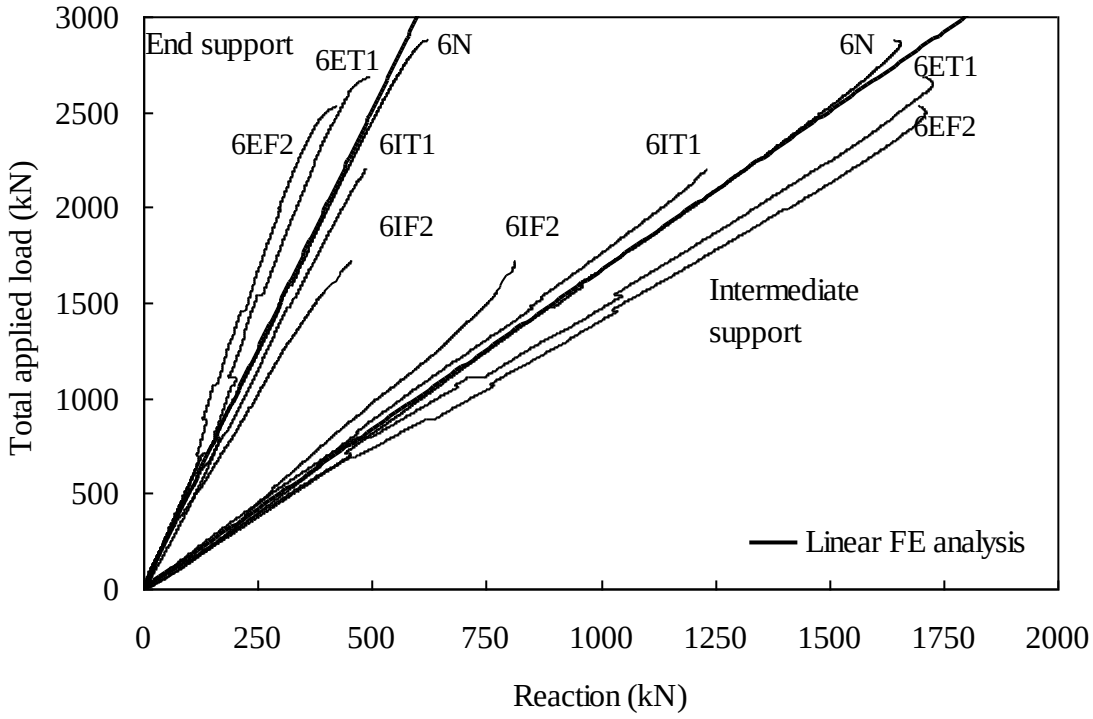

(a) a/h = 0.6

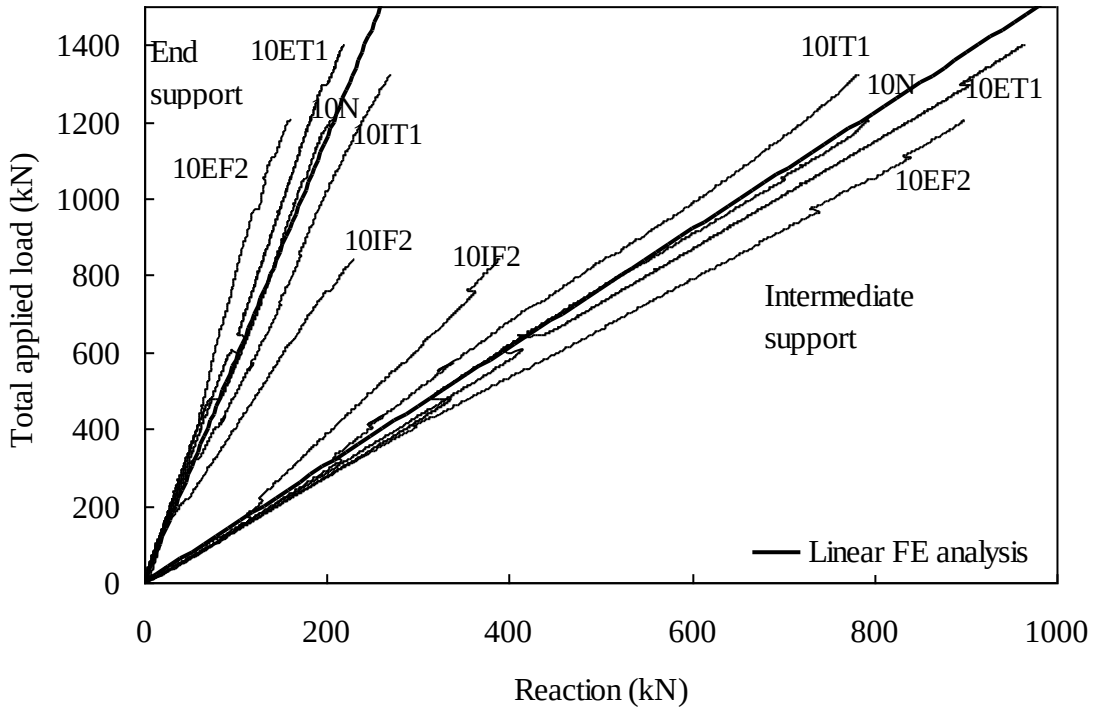

(b) a/h = 1.0

Fig. 6–Support reaction against total load.

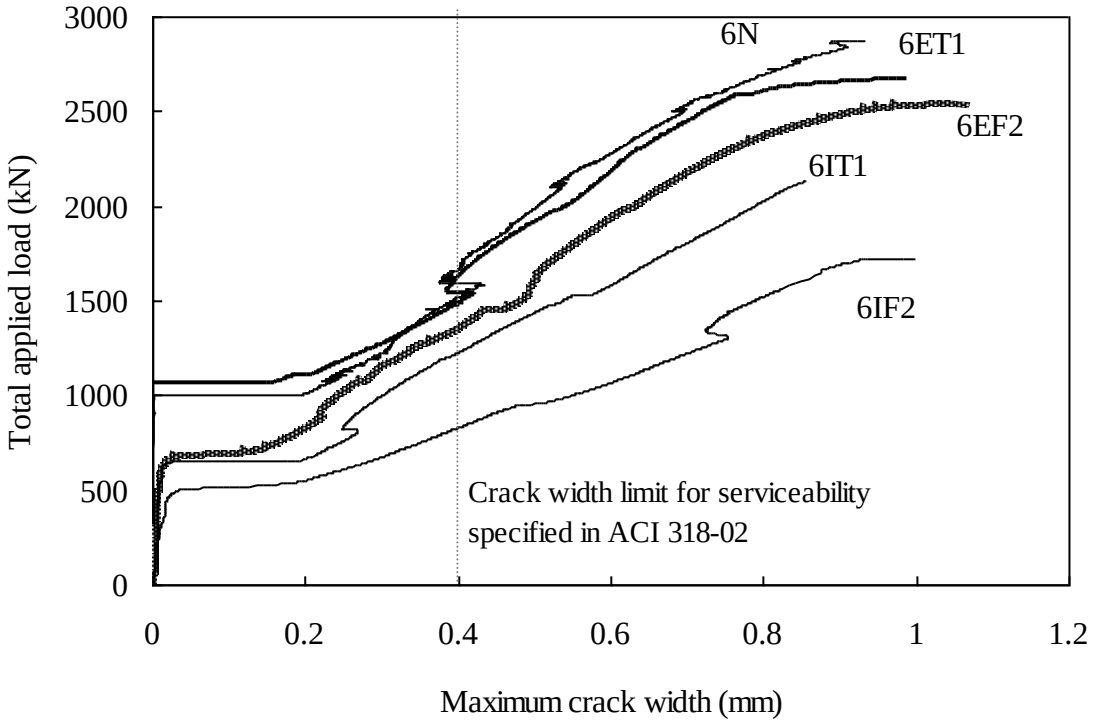

(a) a/h = 0.6

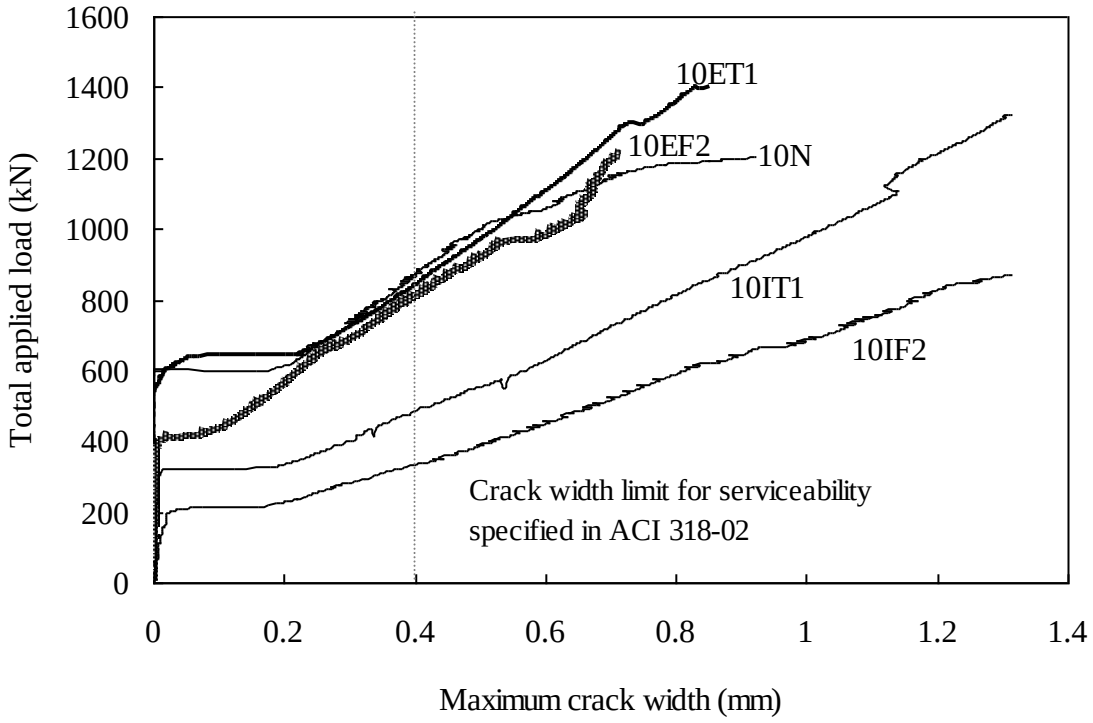

(b) a/h = 1.0

Fig. 7–Maximum diagonal crack width against total applied load.

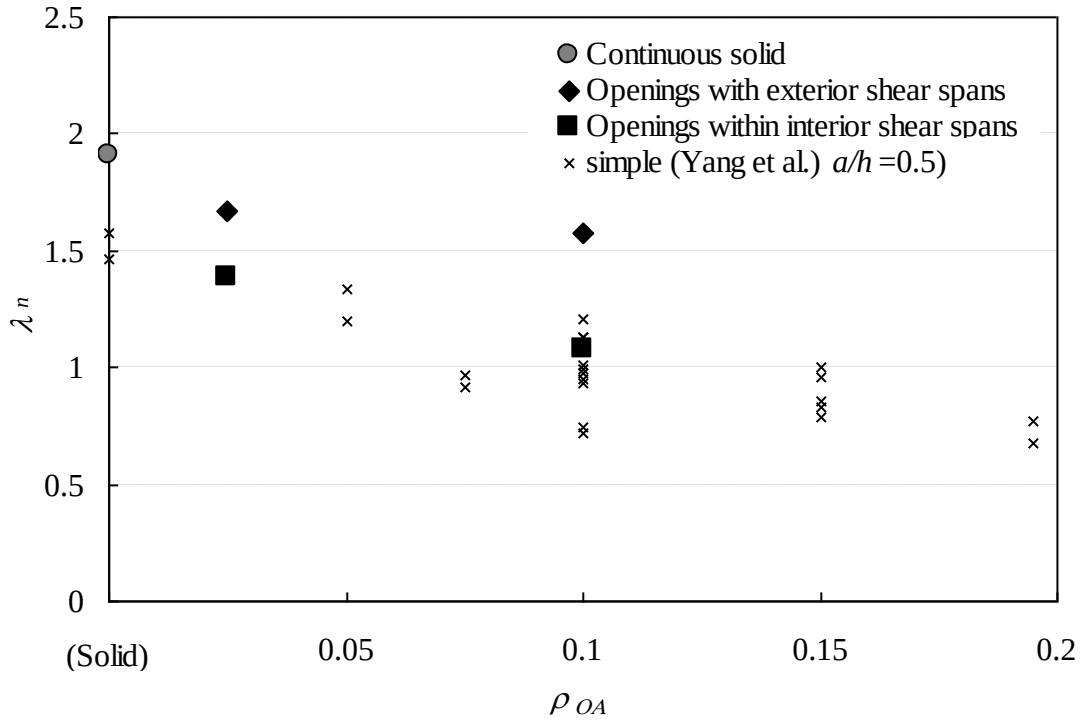

(a) a/h = 0.6

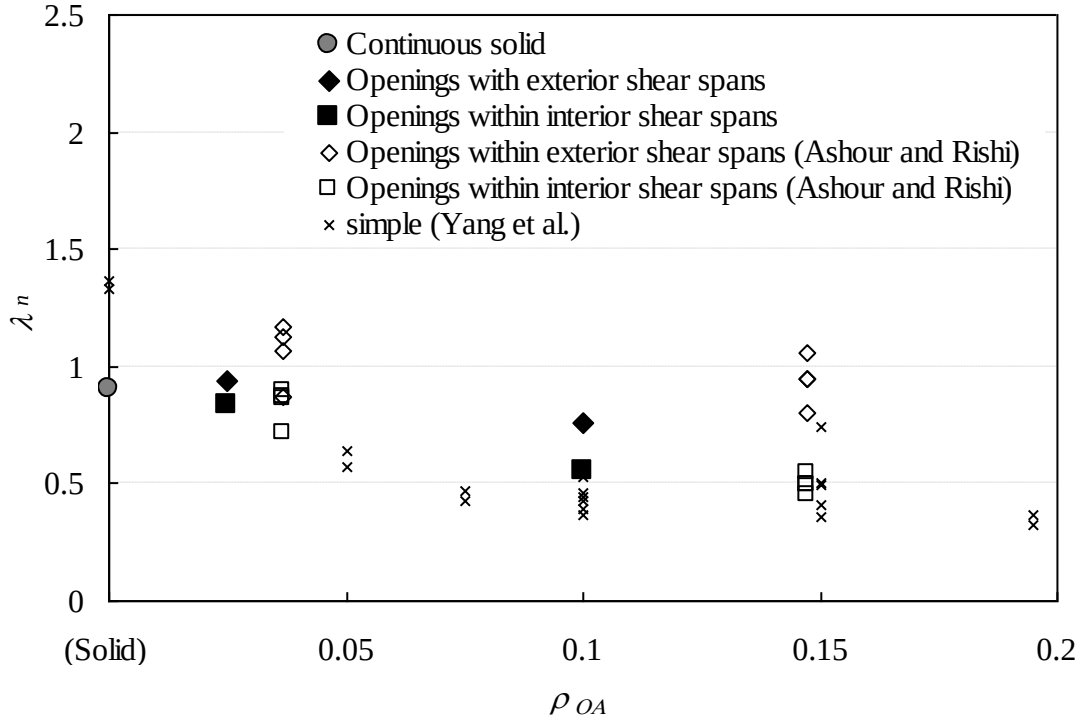

(b) a/h = 1.0

Fig. 8–Relationship between ρ_{OA} and λ_n.

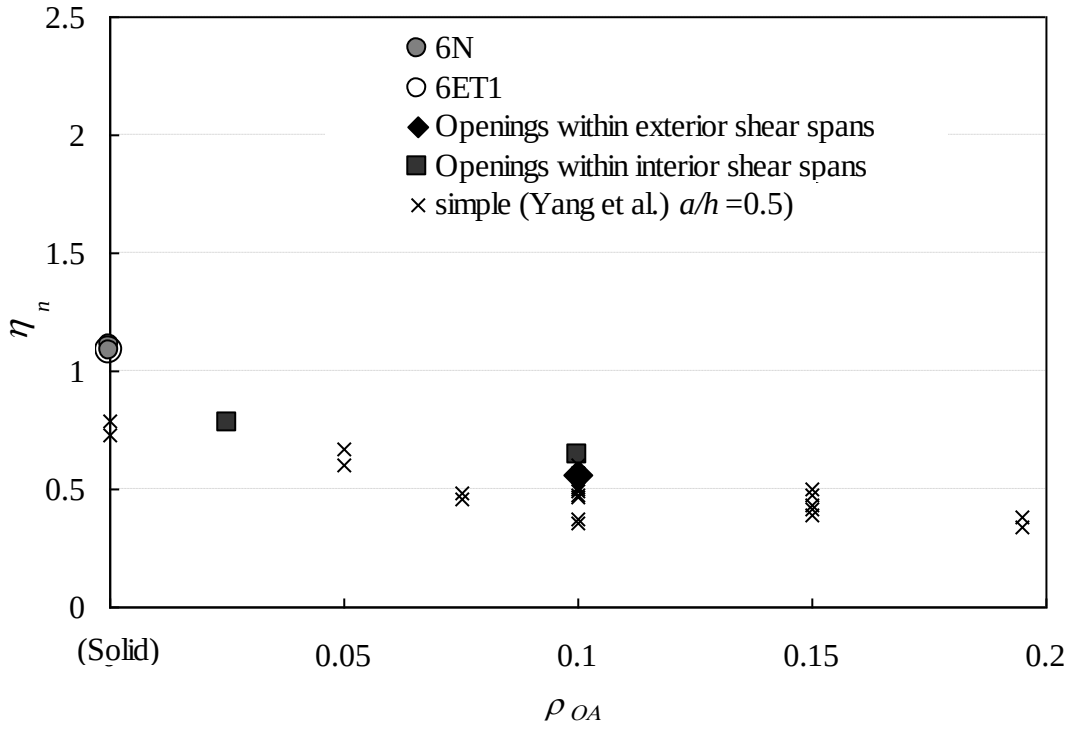

(a) a/h = 0.6

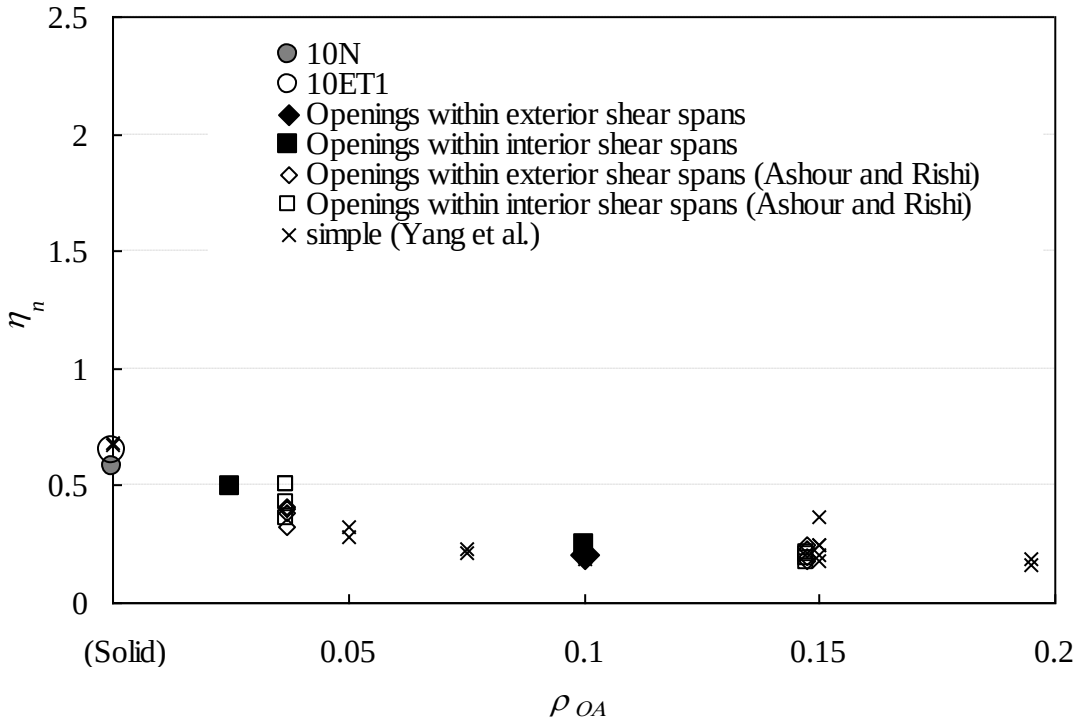

(b) a/h = 1.0

Fig. 9–Relationship between ρ_{OA} and η_n.

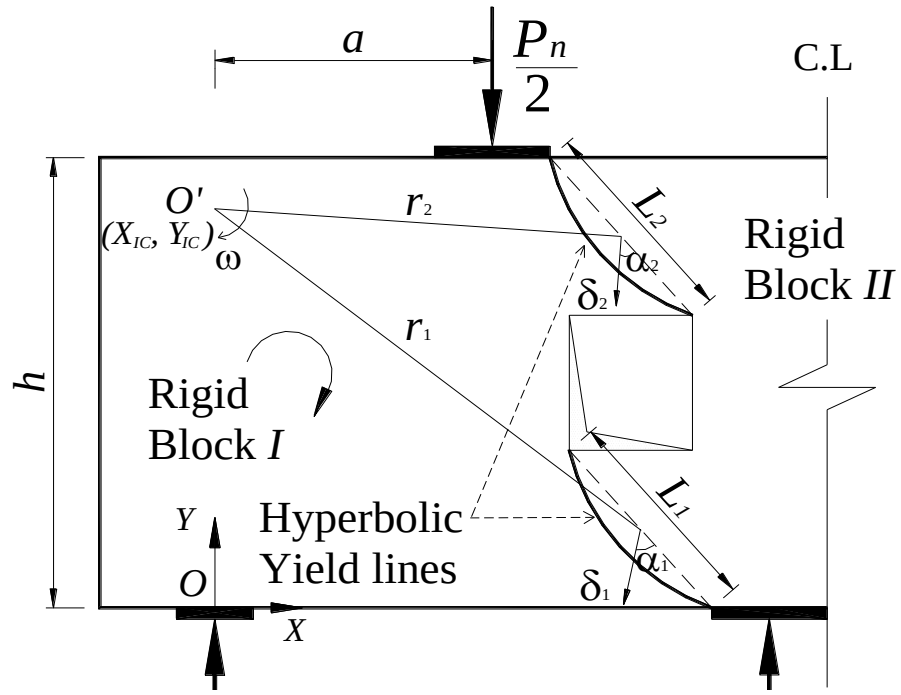

(a) Failure mode A (Beams having web openings within interior shear spans)

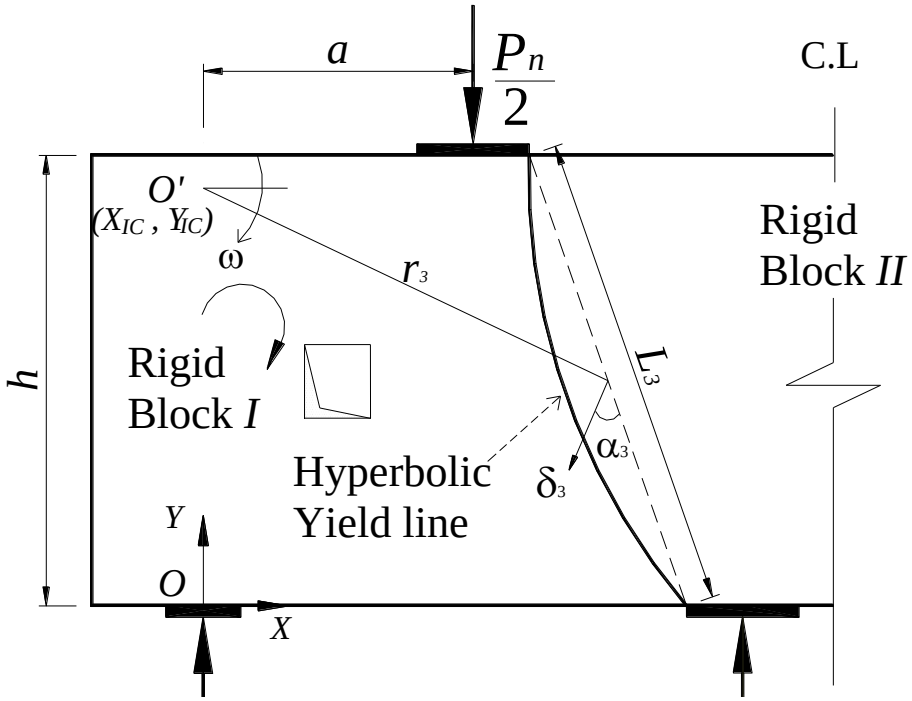

(b) Failure mode A (Solid deep beams or beams with openings within exterior shear spans, of an area ratio ρ_{OA} less than 0.025~0.037)

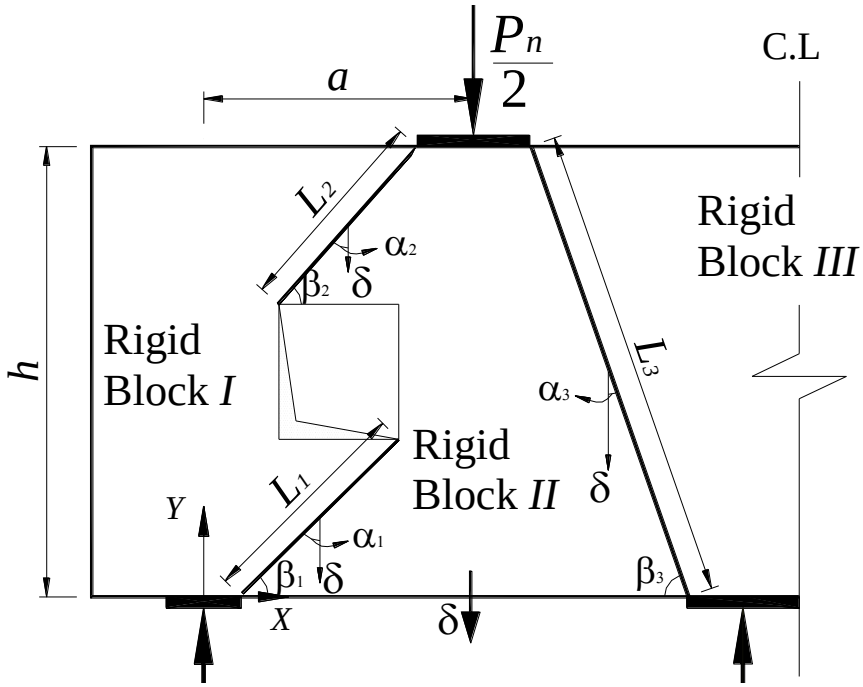

(c) Failure mode B (Beams having ρ_{OA} over 0.037 within exterior shear spans)

Fig. 10–Idealization of failure mechanism for continuous deep beams with web openings.